Semnan University

Mechanics of Advanced Composite Structures

Journal homepage: https://macs.semnan.ac.ir/

ISSN: 2423-7043

Research Article

Quantitative Analysis of the Effect of the Number of Bolt Rows on Shear Strength in Bolted Connections of Fiber-Reinforced Polymer Plates: Comparative Assessment of ASCE/SEI 74-23 and CEN/TS 19101:2022 Design Equations

Mohammad Hossein Imandoust*

Department of Civil Engineering, Yazd University, Yazd, 8915818411, Iran

ARTICLE INFO

Article history:

Received: 2024-10-19
Revised: 2025-03-22
Accepted: 2025-05-12

Keywords:

FRP material;
Bolted connection;
Static tension load;
Shear-out failure;
Strength prediction.

ABSTRACT

Fiber-reinforced polymer (FRP) composites are increasingly employed in structural applications due to their advantageous properties, including a high strength-to-weight ratio and corrosion resistance. Besides FRP bars, FRP profiles and plates are also widely used in the construction industry, and their connection type plays a critical role in the design process. Among the different types of connections for FRP plates, bolted joints are favored for their simplicity and ease of maintenance. This study investigates the influence of the number of bolt rows on the shear-out capacity of double-lap shear bolted connections in FRP plates subjected to static tensile loading. Specifically, the study compares the shear-out capacity predictions derived from two established design standards: ASCE/SEI 74-23 and CEN/TS 19101:2022. The analysis considers configurations with one, two, and three bolt rows, each consisting of a single bolt, thereby avoiding the block-shear failure mode. The results based on CEN/TS 19101:2022 indicate that increasing the number of bolt rows from one to two substantially enhances the joint capacity. However, the inclusion of a third bolt row provides negligible improvement. Conversely, according to ASCE/SEI 74-23, increasing the number of bolt rows consistently enhances the predicted connection capacity. This difference is attributed to the different coefficients used in the corresponding design equations. The findings indicate that geometric parameters, as well as material properties, significantly influence the calculated joint capacity. Furthermore, comparison of the two standards reveals that ASCE/SEI 74-23 tends to produce more conservative estimates of connection capacity than CEN/TS 19101:2022. These differences predominantly arise from the distinct design philosophies and the application of adjustment factors within each standard. Notably, ASCE/SEI 74-23 provides greater safety margins through the incorporation of load type-dependent adjustment factors.

1. Introduction

Fiber-reinforced polymer (FRP) composites constitute a comparatively recent addition to the construction industry. Over the past decades, comprehensive experimental and numerical investigations have substantiated the feasibility of employing FRP composites as effective

* **Corresponding author.**
E-mail address: *mohoimandust@gmail.com*

Cite this article as:

Imandoust, M. H., 2026. Quantitative Analysis of the Effect of the Number of Bolt Rows on Shear Strength in Bolted Connections of Fiber Reinforced Polymer Plates: Comparative Assessment of ASCE/SEI 74-23 and CEN/TS 19101:2022 Design Equations. *Mechanics of Advanced Composite Structures*, 13(1), pp. xxx-xxx.

https://doi.org/10.22075/MACS.2025.39315.2050

substitutes for conventional materials in civil and structural engineering applications. The increasing adoption of FRP composites by the engineering community is largely attributable to their outstanding strength-to-weight ratio, corrosion resistance, and electrical insulation (when glass fibers are used). Nevertheless, FRP composites possess inherent limitations that necessitate careful consideration during design and analysis. Unlike metals, FRP exhibits an essentially linear-elastic response up to rupture, devoid of a yielding plateau under either tensile or compressive loading, thereby resulting in characteristically brittle and abrupt failure [1]. Furthermore, the viscoelastic nature of the polymeric matrix gives rise to time-dependent phenomena, including creep deformation and stress relaxation under sustained loading [1]. Owing to the directional nature of the reinforcing fibers, FRP composites are inherently anisotropic; consequently, their strength, stiffness, and failure mechanisms are profoundly influenced by fiber orientation and laminate stacking sequence. Although commercial pultruded profiles and plates are frequently designed to exhibit near-quasi-isotropic behavior through multidirectional lay-ups (typically incorporating 0°, 90°, and ±45° plies), significant orthotropy persists, particularly in mechanically fastened joints [2]. Among the available connection methods, bolted connections remain predominant in practice owing to their economical installation, rapid assembly, absence of curing requirements, and ease of disassembly. The structural performance of bolted connections in FRP elements is governed by a multitude of interacting parameters in addition to fiber orientation. These parameters include the bolt diameter (d_b), hole clearance (d_h-d_b), end distance parallel to the loading direction (e_1), edge distance transverse to the loading direction (e_2), pitch spacing (s), gauge spacing (g), laminate thickness (t), and the angle (θ) between the principal fiber direction and the applied load [2, 3]. Another critical factor is the joint configuration, namely, single-lap or double-lap. Single-lap joints introduce load-path eccentricity, inducing secondary bending and out-of-plane deformation, which promote localized bearing damage beneath the bolt head or washer and consequently reduce the ultimate load-carrying capacity [5].

When a single bolt is present in a bolt row, the recognized failure modes of bolted FRP connections include net-tension, shear-out, cleavage, and bearing (Fig. 1). Net-tension failure manifests as transverse cracking across the net section and is typically precipitated by an insufficient edge distance (e_2) or by a principal fiber direction oriented perpendicular to the applied load. Shear-out failure involves longitudinal splitting along the loading direction on both sides of the bolt hole and is primarily governed by an insufficient end distance (e_1) and fiber alignment parallel to the applied load. Cleavage failure represents a combination of net-tension and shear-out mechanisms and is commonly observed when both e_1 and e_2 are insufficient, particularly in quasi-isotropic laminates. In contrast, bearing failure develops progressively through the accumulation of localized damage, providing warning before catastrophic failure. Consequently, bearing is generally regarded as the preferred pseudo-ductile failure mode for design purposes [2].

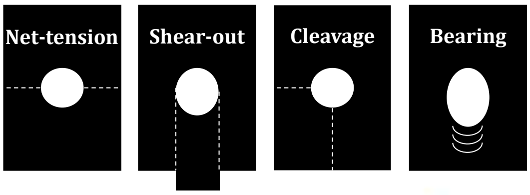

Fig. 1. Types of failure in single-bolted connections [2]

Chamis [6] presented simplified design procedures, illustrated through numerical examples, for estimating failure loads in FRP bolted joints. Notably, the recommended shear-out failure formulation does not account for the influence of bolt-hole clearance on overall connection strength. Hart-Smith [7] developed a specialized stress concentration factor for bolted connections in FRP plates, accommodating their complex mechanical properties. In contrast to isotropic materials, FRP exhibits brittle behavior. Nevertheless, following the initiation of cracks, stress redistribution occurs, yielding a response that deviates from purely elastic or plastic behavior. To accommodate FRP's anisotropy, Hart-Smith introduced a correlation coefficient that establishes a linear relationship between isotropic and anisotropic material responses. Rosner and Rizkalla [8, 9] conducted experimental investigations for geometric variables, including plate width (w), end distance (e), and thickness (t) of the plate. By integrating these empirical data with Hart-Smith's analytical frameworks, they formulated a design protocol for bearing, net-tension, and cleavage failure mechanisms. The influence of geometric parameters, particularly the end distance-to-diameter ratio (e_1/d) and width-to-diameter ratio (w/d), was explored in studies [10–12]. These investigations demonstrate that, for a fixed end distance (e_1), increasing the plate width (w) induces a transition from net-tension to bearing failure. Conversely, maintaining constant plate width while increasing the end distance prompts a shift from shear-out to bearing failure. Lee et al. [13] concluded that clearances exceeding 2 mm exert negligible impact on connection strength. In addition, they proposed that the Eurocomp recommended clearance (0.05 d_b) is impractical for construction applications. Abd-el-Naby and Hollaway [14] advocated for double-bolted configurations as a superior alternative to single-bolted joints, thereby augmenting the tensile capacity of FRP connections. This strategy entails substituting a single bolt with two smaller-diameter bolts, positioned in tandem rows with one bolt each, which enlarges the net cross-sectional area and enhances resistance to net-tension failure. Their observations reveal that the first bolt row carries a larger proportion of the applied load relative to the second row. Ascione et al. [15] investigated the effect of the angle "θ" between fiber alignment and loading direction, affirming its significant influence on bearing failure and offering equations that incorporate "θ" into strength predictions. Loganathan et al. [16] carried out experiments investigating the effect of on-axis and off-axis load directions (relative to fiber orientation) on the tensile strength of composite plates. Samples with off-axis configurations promoted less efficient stress redistribution. Consequently, the inclined fiber arrangement increases stress concentrations and accelerates damage initiation and propagation, resulting in earlier onset of failure and more severe failure mechanisms compared with on-axis specimens. Findings from [17] underscore the criticality of clamping force, especially for crack initiation, as washer-induced pressure on the FRP surface reduces the delamination proximate to the bolt hole, thereby upholding plate integrity within the contact zone. Consequently, fractures propagate beyond this area. However, excessive clamping force may embed the washer, causing load eccentricity and diminishing joint capacity. Gopalan and Narayanan [18] investigated the applicability of blind bolts in box-section FRP profiles, where restricted access renders traditional bolting infeasible. Olivier et al. [19] assessed blind bolt efficacy across diverse loading regimes, including cyclic and sustained static conditions, concluding that such fasteners exhibit diminished capacity to counteract creep-induced degradation. Ghasemi and Moradi [20] investigated the effect of thermal cycling on the durability of polymer matrix composites, observing progressive total mass loss (TML), surface matrix degradation, and deterioration of mechanical properties. They reported that TML increases with the number of thermal cycles, while unnotched laminates exhibit greater mass loss than open hole specimens, with more pronounced surface degradation occurring around hole edges. Furthermore, hole geometry influences degradation behavior, as specimens with lower diameter-to-width ratios experience higher mass loss, highlighting the combined effects of thermal aging and stress concentration on composite performance. Crack repair in fiber-reinforced polymer (FRP) composites has attracted significant attention due to its importance in restoring structural integrity and extending service life. Conventional epoxy resin injection and adhesive repair techniques have been shown to effectively repair matrix cracks and delaminated regions, recovering a substantial portion of the residual flexural strength of damaged composites [21]. More recently, self-healing polymer nanocomposites incorporating nanofillers such as graphene and carbon nanotubes have demonstrated improved crack-healing efficiency, fracture toughness, and damage resistance, offering a promising approach for enhancing the durability and long-term reliability of repaired FRP structures [22].

Gennedy et al. [23] investigated the effect of adding multiwalled carbon nanotubes during the fabrication of unidirectional glass fiber reinforced polymer (GFRP) plates on the shear strength of bolted joints. The experimental investigations showed that incorporating multiwalled carbon nanotubes improved the shear strength, ductility, and energy absorption significantly. Microstructural analysis indicates that a chemical reaction between multiwalled carbon nanotubes and epoxy improves the shear strength of the matrix.

Although extensive research has been conducted on FRP bolted connections, limited attention has been given to comparing the shear-out strength formulations adopted by current design standards. Moreover, the influence of the prescribed adjustment factors and the number of bolt rows on the predicted connection capacity has not been systematically evaluated. This study addresses these gaps through an analytical assessment of the available design approaches.

The present study presents an analytical comparison of the shear-out strength formulations provided in two design standards for FRP bolted connections, ASCE/SEI 74-23 [2] and CEN/TS 19101:2022 [3], and subsequently evaluates the effect of the number of bolt rows on the predicted connection capacity. Furthermore, the influence of the prescribed adjustment factors is also discussed. For the purposes of this analysis, the connection is assumed to be a double-lap shear configuration subjected to static tensile loading.

2. Methodology

The analysis is restricted to double-lap shear connections subjected to quasi-static tensile loading, in which a pultruded FRP plate is sandwiched between two steel cover plates and fastened with a high-strength bolt. As illustrated in Fig. 2, the specimen is mounted in the testing machine using mechanical grips, and the tensile load is transferred through the steel cover plates to the bolted FRP connection.

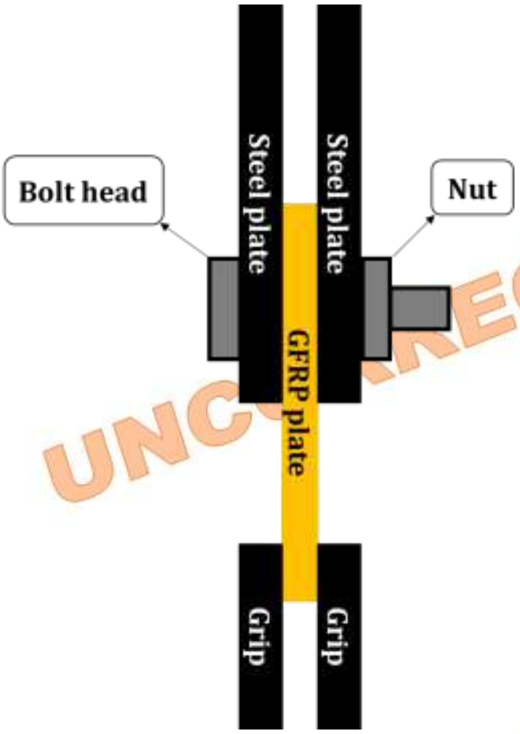

Fig. 2. Double-lap shear connection [4]

All geometric parameters are selected so as to ensure shear-out is the governing failure mode while satisfying the minimum requirements specified in both [2] and [3] (summarized in Fig. 3 and Table 1).

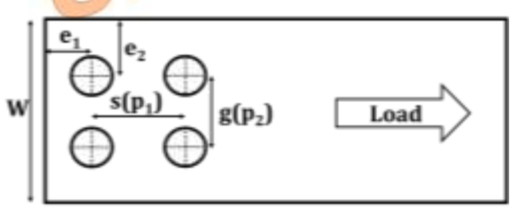

Fig. 3. Connection geometry: pitch spacing (s, p_1), gauge spacing (g, p_2), edge distance (e_2), and end distance (e_1) [2, 3]

To investigate the effect of the number of bolt rows, three connection configurations (Fig. 4) are considered, differing only in the number of bolt rows (n = 1, 2, and 3 for configurations A, B, and C, respectively). Longitudinal pitch (s), end distance (e_1), edge distance (e_2), and plate width (w) are kept constant for all configurations at values that ensure e_1/d and w/d ratios are sufficient to suppress net-tension, cleavage, and bearing failure prior to shear-out. The FRP material properties are adopted from the experimental study by Martins et al. [4], which investigated an E-glass/polyester pultruded plate with unidirectional fiber orientation (θ=0°). The essential properties include: t = 6 mm (plate thickness), $F_{t,L}$ = 734.07 MPa (longitudinal tensile strength), and F_{sh} = 73.33 MPa (in-plane shear strength).

Table 1. Minimum required values of connection geometric parameters [2, 3]

Parameter	ASCE [2]	CEN/TS [3]
Bolt diameter (mm)	$9.53 \le d_b \le 25.4$	$t_{min} \le d_b \le 1.5t_{min}$
Clearance (mm)	1.6	1
End distance (single bolt row)	$e_1 \ge 4d_b$	$e_1 \ge 2.5d_b$
End distance (multi bolt row)	$e_1 \ge 2d_b$	$e_1 \ge \max(2d_b,$ 30 mm)
Edge distance	$e_2 \ge 1.5d_b$	$e_2 \ge 2d_b$
Pitch spacing	$s \ge 4d_b$	$p1 \ge 4d_b$
Gauge spacing	$g \ge 4d_b$	$P2 \ge 4d_b$

In Table 1, t_{min} is the minimum thickness of the FRP plate in the connection.

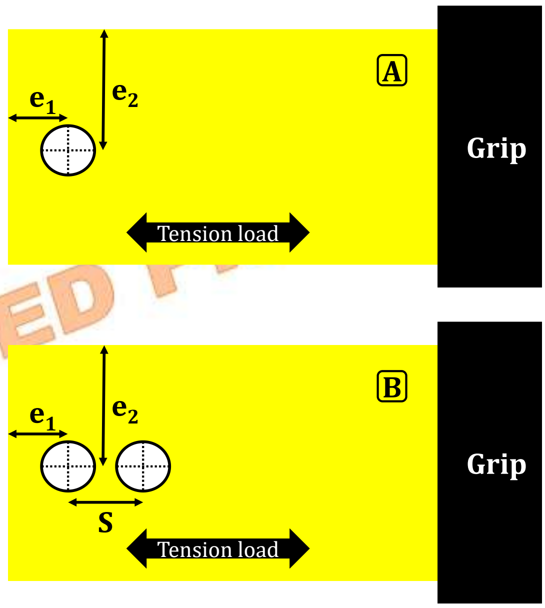

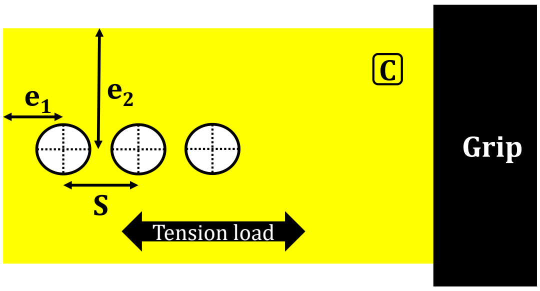

Fig. 4. Sample configurations: single bolt row (A), double bolt row (B), and triple bolt row (C)

The bolt is Grade 10.9, with a shear strength of 650 MPa and a diameter of 10 mm. The bolt diameter is selected to satisfy the minimum requirements specified in both design references. The maximum allowable hole clearance is 1.6 mm according to [2], whereas it is limited to 1 mm in [3]. Therefore, a clearance of 1 mm is adopted in this study to eliminate the influence of different clearance values. Considering the different recommended limits for the end distance, the value of "e_1" is set equal to $3d_b$ to prevent bearing failure of the FRP plate. The steel cover plates are designed with sufficient thickness and material strength to preclude bearing failure of the steel components.

The adjustment factors for connection capacity specified in [2, 3] are summarized in Table 2. The primary differences between the two standards are the time-effect factor (λ) specified in ASCE/SEI 74-23 [2] and the material factor (γ_m) specified in CEN/TS 19101:2022 [3]. The factor "λ" is dependent on the load type and assumes different values for different loading conditions. In the present study, a static loading condition is considered. The factor "γ_m" depends on the method used to determine the material properties. For FRP plates, "γ_m" is equal to 1.15 and 1.5 when standard test results and theoretical equations are employed, respectively.

Table 2. Adjustment factors [2, 3]

Adjustment factor	ASCE	CEN/TS	Explanation
Moisture effect	C_M	η_{CM}	similarity
Temperature effect	C_T	η_{CT}	Similarity
Geometric effect	C_Δ	γ_{RD1}	Similarity
Resistance	Φ	γ_{RD2}	Similarity
Material property	---	γ_m	Material effect
Time effect	λ	---	Considering type of load

The constant parameters for substituting into the formulations of both references are presented in Table 3:

Table 3. Constant geometric parameters of samples

e_1	w	s	d_b (mm)	d_h (mm)	t (mm)	F_{sh} (MPa)
3d	$6d_b$	$4d_b$	10	11	6	73.33

In this study, the connection is assumed not to be exposed to severe chemical or thermal conditions. Therefore, the service temperature is set to 90 °F (32 °C) to minimize its effect on the connection capacity. According to the criteria specified in ASCE/SEI 74-23 [2], the temperature effect should be considered when the service temperature exceeds 32 °C.

The moisture factor in [2] depends on the type of polymer matrix used in the FRP plate, whereas in [3], it is governed by the moisture exposure condition. Considering the assumed environmental conditions (selected to minimize the effect on capacity) and the specified service temperature, the exposure condition is classified as Class II according to Section 2.2 (outdoor exposure without continuous exposure to water).

The shear-out capacity is calculated independently using the respective formulations and adjustment factors specified in ASCE/SEI 74-23 [2] (Section 2.1) and CEN/TS 19101:2022 [3] (Section 2.2). The results are subsequently compared in terms of the predicted ultimate load, the influence of bolt-row multiplicity, and the effect of adjustment factors.

2.1. ASCE/SEI 74-23

According to the formulations presented in ASCE/SEI 74-23 [2], the shear-out strength of bolted connections can be calculated using Eq. (1) for a single bolt row and Eqs. (2) and (3) when there are two and three (n=2 and 3) bolt rows, respectively:

$$R_1 = 1.4\,(e_1 - \frac{dh}{2})\; t\,F_{sh} \qquad (1)$$

$$R_2 = 1.4\,(e_1 - \frac{dh}{2} + s)\; t\,F_{sh} \qquad (2)$$

$$R_3 = 2\,((n-1)\,s)\; t\,F_{sh} \qquad (3)$$

$$R_{final} = R \times \Phi \times C_\Delta \times C_M \times C_T \qquad (4)$$

Here, "d_h" is the hole diameter and "F_{sh}" is the in-plane shear strength of FRP material, which can be determined according to ASTM 5379.[24] Other variables: "e_1", "s", and "t" are already explained.

Now, by substituting the constant parameters (listed in Table 3) into Eqs. (1)–(3), the shear-out strength of the connections can be calculated. Then, to incorporate the adjustment factors, the calculated capacities are substituted into Eq. (4). The adjustment factors are presented in Table 4 for each configuration:

Table 4. Adjustment factors [2]

Sample	λ	Φ	C_Δ	C_M	C_T
A		0.5			
B	0.4	0.45	1	0.8	1
C		0.45			

In Table 4, λ = 0.4 because the applied load is static; Φ= 0.5 for single-bolted connections and Φ=0.45 for multi-bolted connections; C_Δ=1 because $s=s_{min}$; C_M= 0.8 because the polymer matrix in the FRP plate is polyester, and C_T = 0.9 because the service temperature (T_s) is assumed to be 90 °F.

2.2. CEN/TS 19101:2022

In this section, the formulations specified in CEN/TS 19101:2022 [3] are used to calculate the shear-out strength of the investigated connections.

By replacing the constant parameters (Table 3) in Eqs. (5)–(7), the shear-out strength can be determined. Eq. (5) is for a single bolt row, and Eqs. (6) and (7) apply to two and three bolt rows, respectively:

$$R_1 = 1.5\ (e_1 - \frac{d_h}{2})\ t\,F_{xy} \quad (5)$$

$$R_2 = 1.5\ (e_1 - \frac{d_h}{2} + p_1)\ t\,F_{xy} \quad (6)$$

$$R_3 = 1.3\ (i - 1)\ p_1)\ t\,F_{xy} \quad (7)$$

Here, "d_h" is the hole diameter, "i" is the number of bolt rows, and "t" and "p_1" are explained in Table 1. "F_{xy}" is the design value of in-plane shear strength of the FRP plate, which can be calculated by Eq. (8):

$$F_{xy} = (\eta_c \div (\gamma_m \times \gamma_{RD}))\ F_{sh} \quad (8)$$

$$\eta_c = \eta_{CM} \times \eta_{CT} \quad (9)$$

The parameter "F_{sh}" represents the in-plane shear strength and has the same value as that defined in Section 2.1. The ageing effect factor (η_C) is obtained by multiplying the conversion factors for temperature and moisture effects, namely "η_{CT}" and "η_{CM}", respectively. For the calculation of "η_{CT}" (Section 4.4.7.1 of [3]), the glass transition temperature (T_g) is assumed to be 100 °C, while the service temperature (T_s) is taken as 32 °C. Based on the assumed moisture exposure condition (Class II: outdoor exposure without continuous exposure to water), "η_{CM}" is taken as 0.85.

The factor "γ_m" represents the partial safety factor associated with material properties, whereas "γ_{RD}" accounts for uncertainties in the resistance model. According to Section 4.4.5 in [3], since the value of "F_{sh}" is obtained from experimental tests, "γ_m" is assigned a value of 1.15. The value of "γ_{RD}" is taken as 1.5, which is the recommended value for all failure modes of bolted connections according to Table 4.5 presented in Section 4.4.6 of [3]. Therefore, by substituting these parameters into Eq. (8), the design in-plane shear strength of the FRP material is calculated as 31.5 MPa. Subsequently, this value is substituted into Eqs. (5)–(7) to determine the shear-out strength of the investigated connections. The corresponding adjustment factors are presented in Table 5.

Table 5. Adjustment factors [3]

Sample	η_{CM}	η_{CT}	η_C	γ_m	γ_{RD}
A					
B	0.85	0.88	0.75	1.15	1.5
C					

The main difference between the formulations provided in the two references lies in how geometric and environmental effects are incorporated into the calculation of connection capacity. In [2], the shear-out capacity is first calculated and subsequently modified by applying the geometric and environmental factors (C_Δ, C_M and C_T) to the calculated value. In contrast, in [3], the corresponding factors (η_C, γ_m and γ_{RD}) are initially applied to the characteristic in-plane shear strength of the FRP material, which is obtained from coupon tests according to ASTM D5379 [24], to determine the design in-plane shear strength. This design value is then substituted into the corresponding equations to calculate the shear-out capacity.

3. Discussion

3.1. Predicted Capacities

Figure 5 illustrates the calculated connection capacities using the formulations specified in ASCE/SEI 74-23 [2] and CEN/TS 19101:2022 [3] for each connection configuration.

UNCORRECTED PROOF

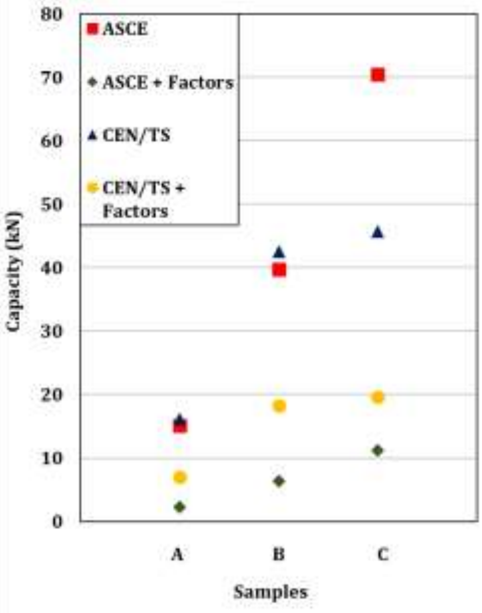

Fig. 5. Comparison of shear-out capacities

In addition, Table 6 presents the percentage differences between the predicted capacities, including the effects of the applied adjustment factors, to facilitate comparison between the two design approaches.

Table 6. Difference comparison of shear-out capacities

Sample	A	B	C	Reference
Capacity (kN)	15.1	39.7	70.4	ASCE
	16.2	42.5	45.8	CEN/TS
Difference (%)	7	7	35	---
Capacity + Factors (kN)	2.3	6.4	11.2	ASCE
	6.9	18.3	19.7	CEN/TS
Difference (%)	65	65	43	---

The results indicate that, before applying adjustment factors, the shear-out capacities predicted by ASCE/SEI 74-23 and CEN/TS 19101:2022 are generally comparable, except for the configuration with three bolt rows, where the ASCE formulation provides a higher prediction. After incorporating the adjustment factors, the capacities calculated according to ASCE remain consistently lower than those obtained from CEN/TS. This indicates that the adjustment factors specified in ASCE provide a more conservative assessment by imposing a greater reduction in the nominal capacity.

For FRP components, the predicted strength of bolted connections is strongly influenced by adjustment factors associated with loading duration, environmental conditions, geometric effects, and uncertainties in the resistance model, resulting in notable differences between the ASCE and CEN/TS approaches. In ASCE/SEI 74-23, a load-type-dependent factor (λ) is introduced to account for creep and other time-dependent effects that reduce the material capacity. In contrast, CEN/TS 19101:2022 incorporates an ageing factor (η_C), which accounts for environmental degradation through the temperature conversion factor (η_{CT}) and moisture conversion factor (η_{CM}). This approach results in a less conservative reduction in strength and consequently higher predicted capacities for similar connection configurations.

Furthermore, CEN/TS distinguishes geometric effects through the factors "γ_{RD1}" and "γ_{RD2}". The factor "γ_{RD1}" accounts for geometric parameters, such as bolt spacing, edge distances, and member dimensions, whereas "γ_{RD2}" represents uncertainties associated with the resistance model, including assumptions related to material properties and failure mechanisms. However, due to the limited experimental data available during the development of CEN/TS, a single general factor (γ_{RD}) was recommended instead of separate factors (γ_{RD1} and γ_{RD2}) for all failure modes of bolted connections. Following the recommendation of CEN/TS, "γ_{RD}" is taken as 1.5 in the present study.

Additionally, according to the CEN/TS predictions, the addition of a third bolt row in Configuration C does not significantly increase the shear-out capacity. Conversely, the ASCE formulation predicts a considerable increase in joint capacity with the addition of the third bolt row. This difference is attributed to the different coefficients adopted in the corresponding design equations.

By comparing the calculated capacities before and after applying the adjustment factors, the reduction associated with each design approach can be quantified. For the ASCE predictions, an 85% reduction in capacity is observed due to the incorporation of adjustment factors, whereas the corresponding reduction for CEN/TS is 57%.

3.2. Validation

In this section, the experimental results for a single-bolted joint reported in [4] and a double-bolted joint in [25] are compared with the calculated capacities obtained using the formulations specified in [2] and [3]. During the experiments, the specimens were not subjected to severe environmental conditions; therefore, the adjustment factors associated with moisture and temperature effects are not considered. For short-term loading under normal environmental conditions, these factors can be neglected. The geometric parameters of the selected specimens are presented in Table 7. It should be noted that the specimens considered in this comparison have a unidirectional fiber orientation (θ= 0).

Table 7. Geometric parameters of specimens

w mm	F_{sh} Mpa	e_1 mm	d_b mm	d_h mm	t mm	s mm
50	73.33	20	8	9	6	---
50	20.2	24	8	9	6.5	32

The comparison for the selected bolt configurations is presented in Table 8.

Table 8. Comparison of analytical and experimental capacity (kN)

Reference	Single bolt [4]	Double bolt [25]
ASCE [2]	9.5	9.5
CEN/TS [3]	10.2	10.2
Experiment	9	12.3

To the authors' knowledge, no previous study was identified during the preparation of this paper that investigated three-bolted joints with the same fiber orientation and failure mode.

3.3. Results

The comparison between the predicted and experimental results indicates that, for the single-bolted connection, the predicted capacities are in close agreement with the experimental values. In contrast, for the double-bolted connection, the addition of a second bolt row increases the level of conservatism, as the calculated capacity is lower than the experimentally measured value. Furthermore, the predictions obtained using the ASCE formulation consistently yield lower capacities than those derived from the CEN/TS formulation, indicating that the ASCE approach provides more conservative estimations.

It should be noted that the database underlying the ASCE standard is more extensive than that used for the development of CEN/TS. The pre-standard version of ASCE was published in 2010, and following 13 years of evaluation, analysis, and comparison with experimental results reported in previous studies, the final standard was developed. In contrast, during the preparation of CEN/TS, as discussed previously, several assumptions were introduced due to the limited availability of experimental data.

The ASCE standard provides a resistance factor, "Φ", for each failure mode, whereas CEN/TS proposes a general resistance factor, "γ_{RD}," for all failure modes. Furthermore, the factors proposed in ASCE consider failure modes based on experimental investigations, while CEN/TS focuses primarily on material properties derived from standard tests. Therefore, for short-term, quasi-static loading under normal environmental conditions, CEN/TS provides less conservative and potentially more economical results. However, for long-term loading and extreme environmental conditions, which introduce considerable uncertainties into structural behavior, the conservative approach adopted by ASCE is considered more reliable.

4. Conclusions

The effect of the number of bolt rows was analytically investigated by comparing the equations presented in two design references for FRP plates and profiles, focusing on the shear-out failure mode under tensile load. Based on the results, the following conclusions can be drawn:

- Uni-directional fiber orientation and parallel applied loading have a significant influence on the occurrence of the shear-out failure mode in bolted joints of FRP plates.
- The primary reason for the differences between the equations presented in the two references is the consideration of geometric and environmental effects.
- The difference in joint capacity predictions without applying adjustment factors is negligible for configurations A and B; however, for configuration C, the ASCE prediction is 35% higher than that of CEN/TS. This difference is attributed to the different coefficients used in the corresponding formulations.
- The adjustment factors specified in ASCE/SEI 74-23 are more conservative than those provided in CEN/TS 19101:2022. The combined value of the factors in ASCE is 0.15, whereas the calculated value in CEN/TS 19101:2022 is 0.43 for the selected geometric and environmental conditions of the samples.
- According to the formulations in CEN/TS, the addition of a third bolt row results in negligible enhancement of the joint capacity, whereas the ASCE formulations predict a significant increase.
- Considering the load-type-dependent factor "λ" specified in ASCE results in a significant reduction in the predicted joint capacity.
- Based on the assumed conditions of the connections investigated in this study, for

short-term, quasi-static loading experiments without severe environmental exposure, the corresponding adjustment factors may be neglected to achieve a more accurate prediction of joint capacity.

- From a design perspective, it is recommended to follow the formulations proposed in ASCE/SEI 74-23 to achieve a safer design that accounts for uncertainties during the construction and service life periods.
- In addition to safety margins, economic considerations should also be taken into account during the design process.
- It should be noted that the conclusions of this study are based on a limited investigation. Therefore, future studies are recommended to extend the comparison to other failure modes, different loading types and rates, and severe environmental conditions to provide a more comprehensive assessment.

Nomenclature

d_b	Bolt diameter
d_h	Hole diameter
e_1	Distance between hole center and free end (for nearest bolt row to the free end)
e_2	Distance between hole center and free edge
s	Pitch spacing, distance between bolt holes parallel to the longitudinal axis of the FRP plate (ASCE)
g	Gauge spacing, distance between bolt holes parallel to the transverse axis of the FRP plate (ASCE)
t	Thickness of FRP member (plate)
t_{min}	Minimum thickness of FRP member (plate)
p_1	Pitch spacing, distance between bolt holes parallel to the length of the FRP plate (CEN/TS)
p_2	Gauge spacing, distance between bolt holes (parallel to the width of the FRP plate (CEN/TS)
F_{sh}	Characteristic in-plane shear strength of FRP material
F_{xy}	Design in-plane shear strength of FRP material.
$F_{t,L}$	longitudinal tensile strength
λ	Time effect factor (depending on load combination)
Φ	Resistance factor
C_{Δ}	Geometry factor
C_M	Moisture condition factor
C_T	Temperature factor
η_c	Conversion factor (considering aging)
γ_m	Partial safety factors related to material properties
γ_{RD1}	Factor accounting for uncertainty of resistance model
γ_{RD2}	Factor accounting for uncertainty of resistance model
γ_{RD}	Overall factor calculated as the product of γ_{RD1} and γ_{RD2}
R	Shear-out strength of connection (calculated from formulas)
i	Number of bolt rows (CEN/TS)
n	Number of bolt rows (ASCE)
T_s	Service temperature

Acknowledgments

This research did not receive any support.

Funding Statement

This research did not receive any specific grant from funding agencies in the public, commercial, or not-for-profit sectors.

Conflicts of Interest

The author declares that there is no conflict of interest regarding the publication of this article.

Appendixes

This research has no appendix.

References

[1] Bank, L. C., 2006. Composite for Construction – Structural Design with FRP Materials. John Wiley & Sons, New Jersey.

[2] ASCE/SEI 74-23, 2023. Load and Resistance Factor Design (LRFD) for Pultruded Fiber Reinforced Polymer (FRP) Structures. Structural Engineers Institute, Reston.

[3] CEN/TS 19101, 2022. Design of Fiber-Polymer Composite Structures, European Committee for Standardization. American Society of Civil Engineers.

[4] Martins, A. D., Seruti, C. A., José Gonilha, Correia, J. A., Teixeira, A. P., Ferreira, F., Silvestre, N., 2025. Shear-out failure of GFRP single-bolted double-lap connections: Experimental investigation and reliability-based code calibration. Composite Structures, Vol. 371:119501.

[5] Smith, P. A.; Pascoe, K. J.; Polak, C. & Stroud, D. O., 1986. The Behavior of Single-lap Bolted Joints in CFRP Laminates. Composite Structures, Vol. 6, No. 3, pp. 41-55.

[6] Chamis, C. C., 1980. Simplified Procedures for Designing Composite Bolted Joints. Forty-third Annual Conference on Fibrous Composites in Structural Design, San Diego, California, New York, Plenum Press, Vol. 9, No. 6, pp. 652-657.

[7] Hart-Smith, L. J., 1987. Mechanically-fastened Joints for Advanced Composites - Phenomenological Considerations and Simple Analyses. Fourth Conference on Fibrous Composites in Structural Design, Plenum, New York, 543-574.

[8] Rosner, C. N. & Rizkalla, S. H., 1995. Bolted connections for fiber-reinforced composite structural members: Experimental program. Journal of Materials in Civil Engineering, Vol.7, No.4, pp.223-231.

[9] Rosner, C. N. & Rizkalla, S. H., 1995. Bolted connections for fiber-reinforced composite structural members: Analytical model and design recommendations. Journal of Materials in Civil Engineering, Vol.7, No.4, pp.232-238.

[10] Cooper, C. & Turvey, G. J., 1995. Effect of joint geometry and bolt torque on the structural performance of single bolt tension joints in pultruded GRP sheet material", Composite Structures, Vol. 32, No. 4, pp. 217-226.

[11] Turvey, G. J., 1998. Single bolt tension joint tests on pultruded GFRP plate- effects of tension direction relative to pultrusion direction", Composite Structures, Vol. 42, No. 4, pp. 341-351.

[12] Wang, Y., 2002. Bearing behavior of joints in pultruded composites. Journal of Composite Materials, Vol. 36, No. 18, pp. 2199-2216.

[13] Lee, Y. G.; Choi, E. & Yoon, S. J., 2015. Effect of geometric parameters on the mechanical behavior of FRP single bolted connections. Composites Part B: Engineering, Vol. 75, pp.1-10.

[14] Abd-el-naby, S. F. M. & Hollaway, L.,1993. The experimental behavior of bolted joints in pultruded glass/polyester material. Part2: Two bolt joints. Composites, Vol. 24, No. 7, pp. 539-546.

[15] Ascione, F.; Feo, L. & Maceri, F., 2009. An experimental investigation on the bearing failure load of glass fiber/epoxy laminates. Composites Part B: Engineering, Vol.40, No. 3, pp.197-205.

[16] Logathan, S. B., Krishnappa, A. K., Kumaravelu, J. C., Bai, G. J., Pavirala, R. & Mathivanan, R., 2025. Effect of ON and OFF Axis Open Hole Tensile Testing of GFRP/Epoxy Composites. Mechanics of Advanced Composite Structures, Vol. 12, No. 25, pp.319-328.

[17] Khashaba, U.A.; Salam, H.E.M.; Al-Shorbagy, A.E. & Seif, M.A., 2006. Effect of washer size and tightening torque on performance of bolted joints in composite structures. Composite Structures, Vol. 73, No.3, pp. 310-317.

[18] Gopalan, R. & Narayanan, P., 2023. Experimental a numerical evaluation of pultruded GFRP double-lap joints with different mechanical fasteners. Results in Engineering, Vol. 18:101035.

[19] Olivier, G.; Csillag, F.; Tromp, E. & Pavlovi´c, M., 2021. Static, fatigue and creep performance of blind-bolted connectors in shear experiments on steel-FRP joints. Engineering Structures, Vol.230, 111713.

[20] Ghasemi, A. R. & Moradi, M., 2017. Open-Hole Size and Thermal Cycling Effects on Mass Loss and Surface Degradation of Polymer Matrix Composites. Mechanics of Advanced Composite Structures, Vol. 4, No. 12, pp.111-116.

[21] Sivagangai, T. & Younus, A. M., 2025. Experimental Investigation of Repair of Glass Epoxy Composite with Edge and Center Crack by Epoxy Resin. Mechanics of Advanced Composite Structures, Vol. 12, No. 25, pp.371-377.

[22] Sharma, S. K., Gajevi´c, S., Sharma, L. K., Sharma, Y. & Sharma, M., 2026. Self-Healing Polymer Nanocomposites: Mechanisms, Structure–Property Relationships, and Emerging Applications. Polymers, Vol. 18. No. 276.

[23] Genedy, M.; Chennareddy, R.; Soliman, E. M.; Kandil, F. U. & Taha, M.R., 2017. Improving shear strength of bolted joints in pultruded glass fiber reinforced polymer composites using carbon nanotubes, Journal of Reinforced Plastics and Composites, Vol.36, No.13, pp.958-971.

[24] ASTM D5379/D5379M-12, 2013. Standard Test Method for Shear Properties of Composite Materials by the V-notched Beam Method, American Society for Testing and Materials, West Conshohocken, PA.

[25] Nhut, P. V., Yoresta, F. S., Duc, T. Q. & Matsumoto, Y., 2024. Strengthening of glass fiber sheets for multi-bolted pultruded GFRP connections: Effect of connection type and bolt-tightening force, Structures, Vol. 65: 106696.